

# Next-to-leading order electron-quark scattering

GJ Kemp<sup>1</sup> and WA Horowitz<sup>2</sup>

<sup>1</sup>Department of Pure and Applied Mathematics, University of Johannesburg, P.O. Box 524, Auckland Park 2006, South Africa

<sup>2</sup>Department of Physics, University of Cape Town, Private Bag X3 Rondebosch 7701, South Africa

E-mail: [gkemp@uj.ac.za](mailto:gkemp@uj.ac.za) & [wa.horowitz@uct.ac.za](mailto:wa.horowitz@uct.ac.za)

**Abstract.** We compute the differential cross section for massless  $2 \rightarrow 2$  scattering between a quark and an electron in a t-channel photon exchange at next to leading order in the  $\overline{\text{MS}}$  renormalisation scheme. Specifically, we show that the result is UV and IR finite. Lastly we explore the role of disconnected contributions to the square of the scattering amplitude.

## 1. Introduction

We compute the differential cross section for massless  $2 \rightarrow 2$  scattering between a quark and electron in a t-channel photon exchange at next to leading order (NLO) in the  $\overline{\text{MS}}$  renormalisation scheme. We couple the quarks to an abelian  $U(1)$  gluon field and compute the NLO calculation in this coupling. We explicitly demonstrate the cancelation of IR-divergences and explore the presence and need for disconnected contributions to amplitude,  $\mathcal{M}$  and to the amplitude squared  $|\mathcal{M}|^2$ . To the best of our knowledge, this calculation has not yet appeared in the literature.

One of the aims of this work is to demonstrate that the cross section at NLO in the coupling is finite. Treatment of the UV divergences are well understood in the context of renormalised perturbation theory. However, there seems to be some controversy involving IR divergence.

Whenever massless particles are present in a theory, one is forced to deal with IR divergences. IR divergences in the vertex correction are indeed cancelled by those arising in real emission processes according to the Bloch-Nordsieck (BN) and Kinoshita-Lee-Nauenberg (KLN) prescriptions [1, 2, 3, 4]. However, there are still real absorption processes to take into account, reintroducing IR divergences. Following KLN, one searches for additional degenerate processes to render the overall process finite. It has been proposed, in the context of the Drell-Yan process and QED electron scattering, to consider contributions from processes involving disconnected gluons and photons [5, 6]. Interference

between these disconnected and connected diagrams at the amplitude level can yield connected contributions at the level of the amplitude squared. While this approach works and the result is again finite, it also lead to disconnected diagrams contributing to the amplitude squared. Indeed, processes involving any number of disconnected photons may contribute to  $|\mathcal{M}|^2$  at the same order of the coupling. To the best of our knowledge this issue has not yet been resolved using the standard techniques of perturbative quantum field theory.

In section 2 we present our results for the leading order and NLO vertex correction. We use dimensional regularisation to regulate all divergences with  $\epsilon \equiv 4 - d$ . Section 3 deals with the real emission process where we present our results for the soft, collinear and soft and collinear real emission processes. Section 4 demonstrates that adding these processes leads to a finite result. Section 5 then explores the issue regarding the disconnected diagrams. Lastly, we only present the divergent pieces of our calculations. We have also computed the finite pieces and are available upon request.

## 2. $2 \rightarrow 2$ scattering at NLO

We compute the following diagrams

$$\begin{array}{c}
 \begin{array}{c} q \xrightarrow{p_i} \text{---} \text{---} \text{---} \xrightarrow{p_f} q \\ \text{---} \text{---} \text{---} \xleftarrow{q_f} e^- \\ \text{---} \text{---} \text{---} \xleftarrow{q_i} e^- \end{array} \\
 + \\
 \begin{array}{c} q \xrightarrow{p_i} \text{---} \text{---} \text{---} \xrightarrow{p_f} q \\ \text{---} \text{---} \text{---} \xleftarrow{q_f} e^- \\ \text{---} \text{---} \text{---} \xleftarrow{q_i} e^- \end{array} \\
 + \\
 \begin{array}{c} \text{---} \text{---} \text{---} \text{---} \text{---} \text{---} \\ \text{---} \text{---} \text{---} \text{---} \text{---} \text{---} \end{array}
 \end{array} \quad (1)$$

for deep elastic scattering. Because the photon momentum in the t-channel exchange is spacelike, it is possible to boost into a frame where energy is conserved. Below, we first compute the leading order diagram, followed by the vertex correction at NLO.

### 2.1. Leading order

The leading order  $\mathcal{M}_0$  amplitude from the LSZ formula in the  $\overline{\text{MS}}$  scheme is

$$\mathcal{M}_0 = \frac{R_{\overline{\text{MS}}}^q R_{\overline{\text{MS}}}^e e^2}{t} \bar{u}(p_f) \gamma^\mu u(p_i) \bar{u}(q_f) \gamma_\mu u(q_i), \quad (2)$$

where  $t$  is a Mandelstam variable. The differential cross section  $d\sigma_0 \propto |\mathcal{M}_0|^2 d\Pi_{LIPS}$ , where where the spin averaging has already been included in  $|\mathcal{M}_0|^2$ . The Lorentz-invariant phase space volume element,  $d\Pi_{LIPS}$ , contains an overall momentum conserving delta function which we use of to evaluate our integrals. The  $R_{\overline{\text{MS}}}$ 's are the residues of the respective two-point functions. In the  $\overline{\text{MS}}$  scheme, the residues are no longer trivial and may be determined from the particle's self energy [7]. In our boosted frame,  $E_{q_i} = E_{q_f}$ , and so the  $\delta$ -function in  $d\Pi_{LIPS}$  may be split up into a spatial part and the temporal part  $\delta(E_{p_i} - E_{p_f})$ . Using the  $\delta$ -functions to evaluate the integrals, the leading order differential cross section

is

$$\left(\frac{d\sigma}{d\Omega}\right)_0 = \frac{(R_{\overline{MS}}^q R_{\overline{MS}}^e)^2 e^4}{16E_{q_i}^4 |v_{p_i} - v_{q_i}|} \left[ 2\left(\frac{\tilde{s}}{\tilde{t}}\right)^2 + 2\left(\frac{\tilde{u}}{\tilde{t}}\right)^2 - \epsilon \right] \left(\frac{E_{p_i}}{2\pi}\right)^{2-\epsilon}, \quad (3)$$

where  $\tilde{s}, \tilde{t}, \tilde{u}$  are Mandelstam variables with unit norm.

## 2.2. Vertex correction

The amplitude for the vertex correction is

$$\mathcal{M}_{v.c.} = R_{\overline{MS}}^q R_{\overline{MS}}^e \frac{\bar{u}(q_f) \gamma^\mu u(q_i) e^2}{t} g^2 \bar{u}(p_f) \gamma^\rho \int \frac{d^d k}{(2\pi)^d} \frac{(\not{p}_i - \not{k}) \gamma_\mu (\not{p}_f - \not{k})}{(p_i - k)^2 k^2 (p_f - k)^2} \gamma_\rho u(p_i). \quad (4)$$

After integrating with respect to the gluon momentum  $k$  and some algebra

$$\mathcal{M}_{vc} = \mathcal{M}_0 \frac{\alpha_g}{4\pi} \left[ -\frac{8}{\epsilon_{ir}^2} - \frac{4}{\epsilon_{ir}} \left( 2 + \log(\tilde{X}) \right) + \frac{2}{\epsilon_{uv}} + \frac{\pi^2}{6} - 8 - 3 \log(\tilde{X}) - \log^2(\tilde{X}) \right], \quad (5)$$

where  $\tilde{X} \equiv 4\pi\tilde{\mu}^2/(-te^\gamma)$ ,  $\gamma$  is the Euler number,  $\tilde{\mu}$  is a scale introduced to make coupling  $g$  dimensionless and  $\alpha_g \equiv \tilde{g}^2/4\pi$ . Lastly, we denoted a positive  $\epsilon$  by  $\epsilon_{uv}$  and a negative  $\epsilon$  by  $\epsilon_{ir}$ . In the  $\overline{MS}$ -bar scheme, the UV-divergence is subtracted out by the counterterm and the scale  $\tilde{\mu}$  is redefined so that  $\tilde{X} = \mu^2/(-t)$ . To the relevant order in  $g$

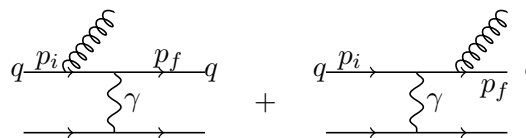
$$R_{\overline{MS}}^q = \frac{1}{1 - \frac{\alpha_g}{2\pi} \frac{1}{\epsilon_{ir}}} \approx 1 + \frac{\alpha_g}{4\pi} \frac{2}{\epsilon_{ir}}. \quad (6)$$

Thus, expanding  $R_{\overline{MS}}^q$ , following the steps in section 2 and simplifying, we obtain

$$\left(\frac{d\sigma}{d\Omega}\right)_{virtual} = \left(\frac{d\sigma}{d\Omega}\right)_0 \left[ 1 + \frac{\alpha_g}{2\pi} \left[ -\frac{8}{\epsilon_{ir}^2} - \frac{1}{\epsilon_{ir}} \left( 6 + 4 \log\left(\frac{\mu^2}{t}\right) \right) + \text{finite} \right] \right]. \quad (7)$$

## 3. Real emission (bremsstrahlung)

The real contributions will fall into two pieces. One will be soft gluon emission from the incoming and outgoing quark lines integrated over all angles, and the other will be from hard collinear gluon emission. For the latter, we treat the case for which the final state gluon is collinear with both incoming and outgoing quark lines. The diagrams are



$$\text{Diagram 1} + \text{Diagram 2} \quad (8)$$

### 3.1. Soft bremsstrahlung

Neglecting the terms that are  $O(k)$  in the numerator, the soft bremsstrahlung amplitude (sb) is

$$\mathcal{M}_{sb} = \mathcal{M}_0 g \left[ \frac{2p_i \cdot \epsilon}{(p_i - k)^2} + \frac{2p_f \cdot \epsilon}{(p_f + k)^2} \right]. \quad (9)$$

The Lorentz-invariant phase space has an extra final state gluon factor and in the soft gluon approximation, we neglect the gluon momentum in the  $\delta$ -function. This leads to the following expression for soft bremsstrahlung differential cross section

$$\left( \frac{d\sigma}{d\Omega} \right)_{sb} = \left( \frac{d\sigma}{d\Omega} \right)_0 \int g^2 \frac{2p_i \cdot p_f}{(p_i \cdot k)(p_f \cdot k)} \frac{d^{d-1}k}{(2\pi)^{d-1} 2\omega_k}. \quad (10)$$

Following [3] in evaluating the integral over all angles and from zero up to some small cutoff gluon energy,  $E_{cut}$ , we find

$$\left( \frac{d\sigma}{d\Omega} \right)_{sb} = \left( \frac{d\sigma}{d\Omega} \right)_0 \frac{\alpha_g}{2\pi} \left[ \frac{8}{\epsilon_{ir}^2} + \frac{4}{\epsilon_{ir}} \log \left( \frac{\mu^2}{\rho E_{cut}^2} \right) + \text{finite} \right], \quad (11)$$

where  $\rho = t/E_{p_i}^2$ .

### 3.2. Hard collinear bremsstrahlung

We consider the final state degeneracy for which the final state gluon is collinear with outgoing quark. According to KLN we also must consider the initial state degeneracy. To account for this, we double our final result.

Beginning from (8), and making use of collinear approximations the hard collinear bremsstrahlung (hcb) differential cross section is

$$\left( \frac{d\sigma}{d\Omega} \right)_{hcb} = \left( \frac{d\sigma}{d\Omega} \right)_0 \frac{\alpha_g}{2\pi} \left[ \frac{1}{\epsilon_{ir}} \left( 8 \log \left( \frac{E_{cut}}{E_{p_i}} \right) + 6 \right) + \text{finite} \right], \quad (12)$$

where ‘finite’ depends on the parameter  $\delta$  - a small angular cutoff below which the detector cannot distinguish between a quark and a quark plus gluon.

## 4. The final result is finite

In this section, we show that the total differential cross section is independent of  $\epsilon_{ir}$  and thus finite as  $d \rightarrow 4$ . Firstly, the  $1/\epsilon_{ir}^2$  terms cancel straightforwardly. Thus, we only have to show that the  $1/\epsilon_{ir}$  terms cancel. For  $\rho = t/E_{p_i}^2$ , we find

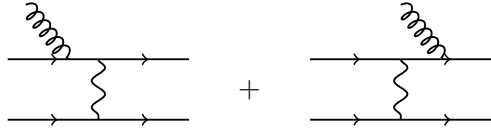
$$\frac{\alpha_g}{2\pi} \frac{1}{\epsilon_{ir}} \left[ -6 - 4 \log \left( \frac{\mu^2}{t} \right) + 4 \log \left( \frac{\mu^2}{\rho E_{cut}^2} \right) + 8 \log \left( \frac{E_{cut}}{E_{p_i}} \right) + 6 \right] = 0. \quad (13)$$

## 5. Disconnected cross sections

In this section, we demonstrate how to cancel the IR-divergences that result from the absorption of a soft gluon by each quark. We reproduce the results of [5, 6] but in the context of our calculation. Searching for additional degenerate processes, we are lead to Feynman diagrams featuring a single disconnected gluon line contributing to  $\mathcal{M}$ . In so doing, we obtain contributions to  $|\mathcal{M}|^2$  from diagrams with disconnected gluon lines. It is not yet clear if this issue may be resolved using standard techniques of perturbative quantum field theory.

We note that very soft massless particles have broad wave packets. It is thus possible for a disconnected gluon's wave packet to overlap with the particles participating in the scattering experiment. Secondly, one can usually rely on the Cluster Decomposition principle to argue that disconnected diagrams need not be considered [8]. However, one can show that the interference between two well-separated collections of fields in a Green's function decays as  $e^{-mR}$ , where  $R$  is the spacelike separation between the two sets of fields and  $m$  is the smallest mass in the theory [9]. For massless particles, this suggests that it is possible to have interference.

The absorption diagrams we compute are

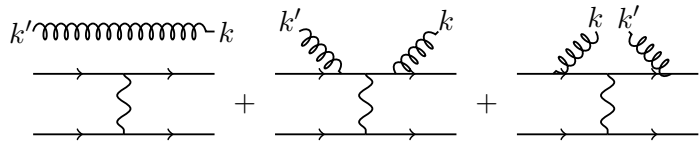


$$(14)$$

The result of this process is the same as the real emission process in section 3.1,

$$|\mathcal{M}_{sb}|^2 = |\mathcal{M}_0|^2 g^2 \frac{2p_i \cdot p_f}{(p_i \cdot k)(p_f \cdot k)}. \quad (15)$$

Once again, we have IR divergences that presumably need cancelling. Now consider the  $3 \rightarrow 3$  processes



$$(16)$$

There are additional diagrams that ultimately evaluate to zero in the massless limit. The first diagram is equal to  $\mathcal{M}_0(2\pi)^3 2\omega_k \delta^{(3)}(k - k')$ . At the level of the amplitude squared, interference between the first diagram and the second two higher order diagrams produces connected contributions to  $|\mathcal{M}|^2$  at order  $e^4 g^2$ . These ultimately lead to  $-2|\mathcal{M}_{sb}|^2$ . KLN states that we should continue to search for additional degenerate processes at  $O(e^4 g^2)$ . It

turns out there are such processes in the degenerate  $3 \rightarrow 4$  scattering amplitude,

$$\begin{array}{c}
 k_2' \text{ wavy line} - k_2 \\
 \text{---} \text{ wavy line} - k_1 \\
 \text{---} \text{ fermion line} \text{---} \\
 \text{---} \text{ fermion line} \text{---}
 \end{array}
 +
 \begin{array}{c}
 k_2' \text{ wavy line} - k_2 \\
 \text{---} \text{ fermion line} \text{---} \\
 \text{---} \text{ wavy line} - k_1 \\
 \text{---} \text{ fermion line} \text{---}
 \end{array}
 \quad (17)$$

with two additional diagrams having  $k_1$  and  $k_2$  swapped. Again, interference occurs between these diagrams to produce a connected contribution to  $|\mathcal{M}|^2$ . The interference turns out to be  $|\mathcal{M}_{sb}|^2$ , precisely what is required to cancel the infrared divergences.

It only remains for us to explain (or explain away) the additional disconnected terms in  $|\mathcal{M}|^2$ . For example, in (16), the leading order  $e^4$  contribution to  $|\mathcal{M}|^2$  features a completely disconnected gluon line. Indeed, one can have any number of disconnected gluon lines and still be at the same order in the coupling.

## 6. Discussion

We have computed the differential cross section for massless  $2 \rightarrow 2$  scattering between a quark and electron in a t-channel photon exchange at next to leading order (NLO) in the  $\overline{\text{MS}}$  renormalisation scheme. We considered the abelian gluon case, and, using dimensional regularisation, we have shown that the cross section is finite. We have also computed (but not shown) the finite pieces to the individual processes. We have briefly explored the role of disconnected diagrams to the amplitude-squared in the context of our specific calculation. We have explained that by opening the Pandora's box of disconnected diagrams, one could, in principle, have to sum an infinite number of disconnected diagrams, all contributing to the amplitude squared at the same order in the coupling.

Acknowledgments:

WH would like to thank SA-CERN and the NRF. GK would like to thank SA-CERN and the UJ GES Postdoc Fellowship.

## References

- [1] Kinoshita T 1962 Mass singularities of Feynman amplitudes *J. Math. Phys.* Volume **3** Number 4 pages 650-677
- [2] Lee T D and Nauenberg M 1964 Degenerate systems and mass singularities *Phys. Rev.* **133** B1549
- [3] Contopanagos H F 1990 Smooth massless limit of QED *Nucl. Phys. B.* **343** 571
- [4] Gastmans R, Verwaest J and Meuldermans R 1976 Dimensional regularization in massless QED *Nucl. Phys. B.* **105** 454
- [5] Akhoury R, Sotiropoulos M G and Zakharov V I 1997 The KLN theorem and soft radiation in gauge theories: abelian case *Phys. Rev. D.* **56**, 377
- [6] Lavelle M and McMullan D 2006 Collinearity, convergence and cancelling infrared divergences *JHEP* **0603** 026
- [7] Srednicki M 2007 *Quantum Field Theory* Cambridge University Press
- [8] Weinberg S 1995 *Quantum Theory of Fields, Volume 1, Foundations* Cambridge University Press
- [9] Brown L S 1994 *Quantum Field Theory* Cambridge University Press